

Harmonic Modeling of Inrush Current in Core Type Power Transformers using Hartley Transform

M. A. Taghikhani^{*(C.A.)}, A. Sheikholeslami^{**} and Z. Taghikhani^{***}

Abstract: This paper presents a new method for evaluation and simulation of inrush current in various transformers using operational matrices and Hartley transform. Unlike most of the previous works, time and frequency domain calculations are conducted simultaneously. Mathematical equations are first represented to compute the inrush current based on reiteration and then Hartley transform is used to study harmonic effects in the frequency domain. Being a real valued function and accordingly giving results with the higher speed of calculations are the main features of Hartley transform. The inrush problem is initially solved for single-phase transformers for switching at different angles of the voltage waveform using this method and then the results of harmonic domain are compared with that of Fourier transform. The methodology is also applied to three-phase three-limb transformers since the analysis of their transient behavior is significant owing to the flux coupling interactions in multi-leg core structures. The feasibility and efficacy of the method is illustrated with appropriate circuits and MATLAB code is developed to get the time and frequency domain waveforms with high accuracy. The results are helpful to identify and evaluate inrush current harmonic effects in various transformers and hence the efficiency of the method is verified.

Keywords: Harmonic Domain, Hartley Transform, Operational Matrices, Transformer Inrush Current.

1 Introduction

Power transformers are sensitive components in power distribution and transmission systems. When a transformer is energized, it will often draw a nonsymmetrical magnetizing current, referred to as inrush current which has particularly undesirable effects on the windings and may gradually ruin the transformer. Large inrush current will be created when the transformer operates on no-load energizing condition. It involves a large and long lasting dc component, which is rich in harmonics, assumes large peak values at the beginning about 6 to 30 times of the rated value. The magnitude of the inrush current drawn by a transformer depends on the source strength, the leakage impedance

and design of the transformer, the residual flux stored in the transformer's core, and the angle of the applied voltage at the time of energization [1-3].

Inrush phenomenon is of nonlinear nature and can only be reproduced by actual tests and computer simulations. Due to the non-linear nature of inrush phenomenon it must be solved by iteration [4]. The authors of [5] used a Newton-type algorithm to solve the inrush problem and a single evaluation of the Jacobian matrix was shown to be most efficient. The method can represent the coupling effects between different harmonic frequencies and the full inrush solution is obtained in a single one harmonic domain iterative solution, i.e., 4-5 Newton iterations. The effects of various parameters such as switching angle and residual flux on the inrush current of a single-phase transformer are investigated in [6] and the second harmonic content of the inrush current is also evaluated. Different Fourier techniques were proposed in [7, 8] to obtain the magnitude and phase angles of the inrush current harmonic component at different voltage angles. The methods are helpful to estimate harmonic effects for inrush current but as the Fourier transform is a complex tool, it requires numerous complex quantities and multiplications. An effective and full frequency

Iranian Journal of Electrical & Electronic Engineering, 2015.

Paper first received 1 Dec. 2014 and in revised form 7 Apr. 2015.

* The Author is with the Department of Engineering, Imam Khomeini International University, Qazvin, Iran.

** The Author is with the Department of Electrical and Computer Engineering, Babol (Noshirvani) University of Technology, Babol, Iran.

*** The Author is with the Department of Electrical and Computer Engineering, Mazandaran University of Science and Technology, Babol, Iran.

E-mails: taghikhani@eng.ikiu.ac.ir, asheikh@nit.ac.ir and zahra.taghikhani@ustmb.ac.ir.

domain solution technique which solves the inrush phenomenon using operational matrices has been developed, assuming that the overall transient is part of a periodic train of transients [4]. This is shown in Fig. 1 where the transient inrush has a period of $2l$ in the time domain. The methodology uses operational matrices and a given orthogonal set, e.g., Hartley series but it takes considerable computation time using large matrices and consequently reduces memory efficiency. Actually, Hartley series are frequently used for periodic signals which are infinite, but the Hartley transform can be applied to approximate the continuous transform of a non-periodic signal of finite duration. It also appears to be a good method of transforming data into the frequency domain, accordingly it is an ideal tool to solve inrush current problem.

A MATLAB code is developed in this paper to get the time and frequency domain waveforms of single-phase and three-phase three-limb transformers inrush currents and their hysteresis loops using operational matrices and Hartley transform. Requiring less number of computations and performing simultaneous calculations in the time and frequency domain are the main features of this technique.

The paper is organized as follows: Section 2 is dedicated to description of operational matrices and explanation of its applications. Relevant equations for Hartley transform and series are given in section 3. The method is applied to the investigation of single phase transformers and three-phase three-limb transformers respectively in section 4 and the simulation results are presented. Section 5 concludes the paper lastly.

2 Operational Matrices

Algebraic methods can be applied to calculate steady state solutions of linear, time-varying and nonlinear systems. They have been established for the solution of problems described by linear differential equations, such as analysis, model reduction, optimal control and system identification. These methods provide identical solutions but they have different numerical properties [4, 9]. In the last four decades, Numerical methods based on operational matrices (especially for orthogonal polynomials and functions) have received considerable attention for dealing with a huge size of applied mathematics problems.

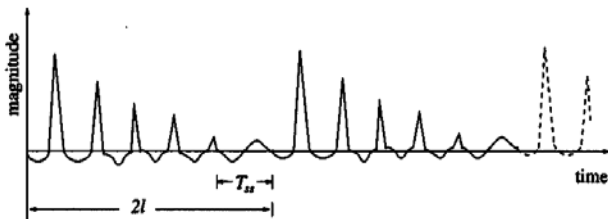


Fig. 1 Transient response seen as a periodic function.

The aim of these techniques is to simplify the solution process of the problem and obtain effective algorithms that are suitable for digital computers [10]. Operational matrices can be applied to various problems such as time and frequency domain analysis. Using algebraic integration of differential equations based on orthogonal calculations of functions simplifies the solution process of the problem in this paper.

3 Hartley Transform and Series

The Hartley transform is an alternate means of analyzing a given function in terms of its sinusoids. This transform is its own inverse and an efficient computational tool where the data are purely real [11]. The Hartley transform of a function is a spectral transform and can be obtained from the Fourier transform by replacing the exponential kernel $\exp(-j\omega t)$ by $\text{cas}(vt)$. Fourier transform for $g(t)$ is:

$$F\{g(t)\} = G(\omega)$$

$$G(\omega) = \frac{1}{\sqrt{2\pi}} \int_{-\infty}^{+\infty} g(t) e^{-j\omega t} dt \quad (1)$$

Hartley transform for $g(t)$ is:

$$H\{g(t)\} = G(v)$$

$$G(v) = \frac{1}{\sqrt{2\pi}} \int_{-\infty}^{+\infty} g(t) \text{cas}(vt) dt \quad (2)$$

The Hartley transform of the derivative of $g(t)$ is:

$$H\left\{\frac{dg(t)}{dt}\right\} = -v G(-v) \quad (3)$$

This transform doesn't convert input signals into their complex exponential and works basically on the principal of even and odd part of signal. A periodic function $f(t)$ of period $2l$ can be approximated by Hartley functions as,

$$f(t) = \sum_{n=-\infty}^{\infty} C_n \text{cas}(nv_0 t) \quad (4)$$

where

$$\text{cas}(nv_0 t) = \cos(nv_0 t) + \sin(nv_0 t) \quad (5)$$

$$v_0 = 2\pi f_0 \quad (6)$$

$f_0 = \frac{1}{2l}$ [Hz] is the frequency in hertz and:

$$C_n = \frac{1}{2l} \int_0^{2l} f(t) \text{cas}(nv_0 t) dt \quad (7)$$

4 Inrush Current Calculation

The methods been used for simulation of transformer inrush current have been almost done for the first peak and most of these procedures have been also performed in the time domain, but due to the nature

of inrush current and existence of harmonics with different orders, it is necessary to consider the inrush current harmonic components. Equations are first represented in the time domain and then the Hartley transform is applied to the equations in this method. The problem should be solved by iteration due to the nonlinear nature of inrush phenomenon and this procedure continues until an acceptable solution is achieved. When the winding is energized at a point different from the voltage peak, a flux equivalent to the remanent flux will appear. Considering this principle, inrush current is calculated for single-phase and three-phase three-limb transformers in this paper.

4.1 Single-Phase Transformers

The unloaded single-phase transformer equivalent circuit used to calculate inrush current is shown in Fig. 2. The inrush current (i_{inr}) may flow in the primary circuit under no load condition. The inrush current transient during the energization of a transformer is a nonlinear phenomenon and the nonlinear characteristic is represented by the following polynomial [4],

$$i_{\psi}(t) = 0.7576 \psi(t) + 1.03 \times 10^7 \psi^{19}(t) \quad (8)$$

Equations below describe the circuit in Fig. 2.

$$v_s(t) = r_1 i_{inr}(t) + L_1 \frac{di_{inr}(t)}{dt} + v(t) \quad (9)$$

$$i_{inr}(t) = \frac{v(t)}{r_{mag}} + i_{\psi}(t) \quad (10)$$

In the nonlinear element,

$$v(t) = \frac{d\psi(t)}{dt} \quad (11)$$

where $v(t)$ is the instantaneous voltage applied to the transformer primary and $\psi(t)$ is the instantaneous core flux of the winding. Discretization of the above equations in the time domain under no-load condition gives:

$$v_s(t) = r_1 i_{inr}(t + \Delta t) + L_1 \frac{i_{inr}(t + \Delta t) - i_{inr}(t)}{\Delta t} + \frac{\psi(t + \Delta t) - \psi(t)}{\Delta t} \quad (12)$$

$$i_{\psi}(t) = i_{inr}(t + \Delta t) - \frac{1}{r_{mag}} \frac{\psi(t + \Delta t) - \psi(t)}{\Delta t} \quad (13)$$

$$\begin{bmatrix} r_1 \Delta t + L_1 & 1 \\ 1 & \frac{-1}{r_{mag} \Delta t} \end{bmatrix} \begin{bmatrix} i_{inr}(t + \Delta t) \\ \psi(t + \Delta t) \end{bmatrix} = \begin{bmatrix} v_s(t) \Delta t + L_1 i_{inr}(t) + \psi(t) \\ i_{\psi}(t) - \frac{\psi(t)}{r_{mag} \Delta t} \end{bmatrix} \quad (14)$$

Representation of these equations in the frequency domain and assuming that $i_{inr}(0) = 0$, gives:

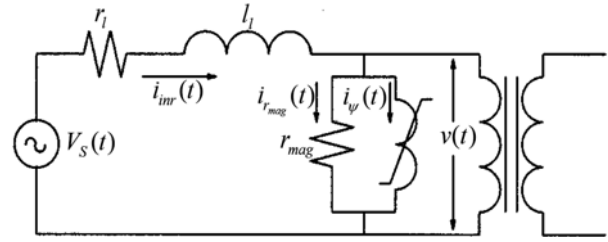


Fig. 2 Single-phase transformer equivalent circuit.

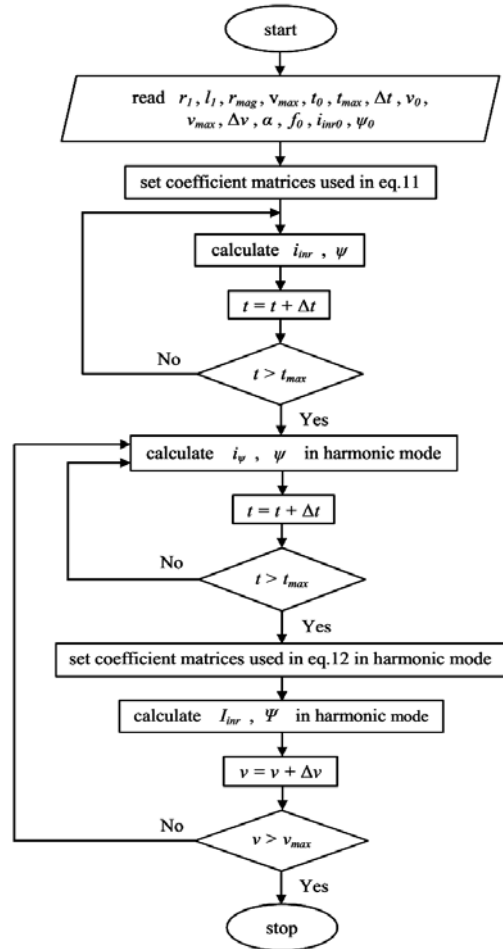


Fig. 3 Flowchart for simulation of inrush current.

$$\begin{bmatrix} r_1 + L_1 v & v \\ 1 & -\frac{v}{r_{mag}} \end{bmatrix} \begin{bmatrix} I_{inr}(v) \\ \Psi(v) \end{bmatrix} = \begin{bmatrix} \int v_s(t) (\cos(vt) + \sin(vt)) dt + \psi(0) \\ \int i_{\psi}(t) (\cos(vt) + \sin(vt)) dt - \frac{\psi(0)}{r_{mag}} \end{bmatrix} \quad (15)$$

The flowchart of the proposed algorithm is illustrated in Fig. 3. Both of time and harmonic domain procedures using the above equations are depicted in this flowchart.

The nonlinear characteristic is considered perfectly in the unloaded single-phase transformer model and core losses can also be evaluated. MATLAB code is used to perform simulations. For this study the

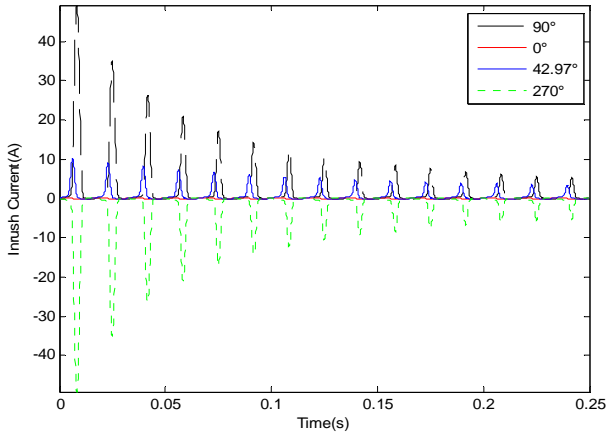


Fig. 4 Inrush current in the time domain at different switching angles.

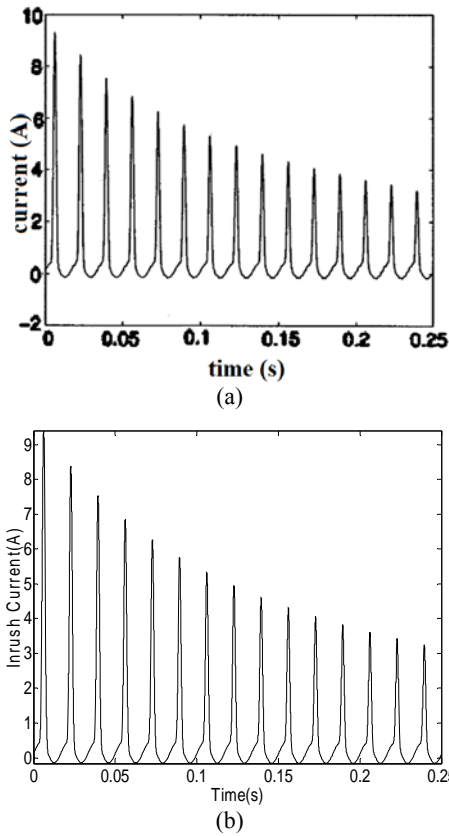


Fig. 5 Inrush current at $\alpha = 42.97^\circ$ using (a) method presented in [4], (b) proposed method.

following parameters are selected [4], $t_{max} = 0.25\text{Sec}$, $S = 1500\text{ VA}$, $f = 60\text{ Hz}$, $V_s = 110\cos(\omega_0 t - \alpha)$, $r_1 = 0.192\ \Omega$, $l_1 = 0.9\text{ mH}$, $r_{mag} = 612.86\ \Omega$.

Fig. 4 shows inrush current in the time domain at different voltage angles under zero residual flux condition.

When the switching takes place at zero of the voltage waveform ($\alpha = 90^\circ$), the inrush current of the transformer's primary winding is at the maximum value.

Switching at the voltage peak ($\alpha = 0^\circ$) causes no saturation in the transformer, and thus, we don't detect the inrush current. Only rated magnetizing current exists in this case. The inrush currents obtained for 42.97° using the method presented in [4] and the proposed method are also shown in Fig. 5 and so the efficacy of the proposed method can be observed. When the angle is 270° , results are the same as 90° but the inrush current possesses the maximum negative value as the switching takes place in the next half cycle. Due to the deep saturation of transformer in these two angles, considerable asymmetries in their hysteresis loops are observed and shown in Fig. 6. The second curve in this figure shows the hysteresis loop for 0° , where the loop is perfectly symmetrical. This method is also compared with the result of inrush current versus time in Matlab Simulink for 90° (which is the worst angle for inrush current) in Fig. 7. It can be observed that both results are exactly the same but simulating via Matlab code gives results with much higher speed.

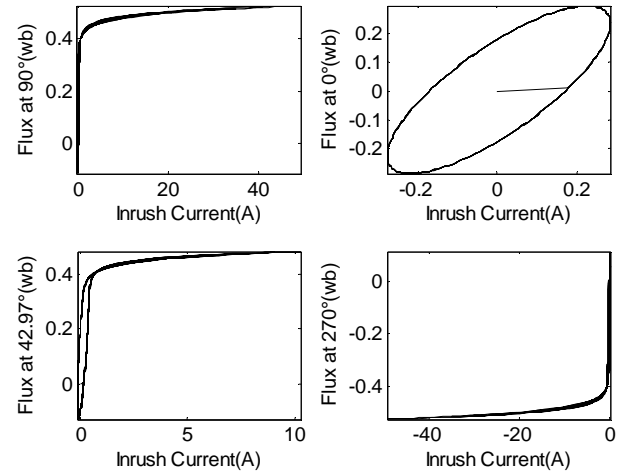


Fig. 6 Hysteresis loops for switching at $\alpha = 90^\circ, 0^\circ, 42.97^\circ$ and 270° .

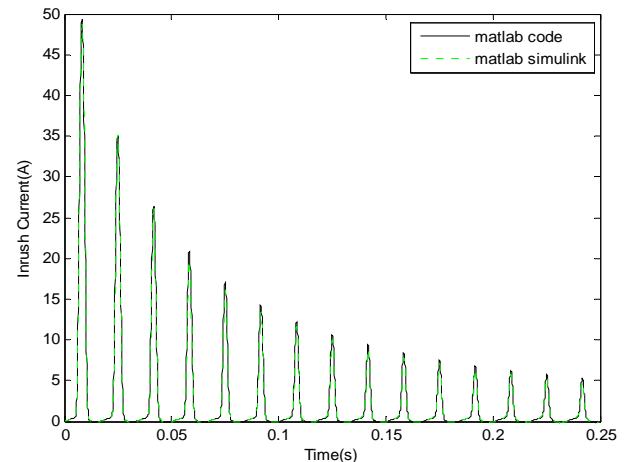


Fig. 7 Comparison between inrush currents obtained at 90° using Matlab code and Simulink.

The harmonic spectrums obtained using operational matrices and Hartley transform are shown in Fig. 8. The fundamental harmonic content of inrush current is the only term which can be observed in this figure for 0° . A significant point about transformer inrush current is the presence of harmonics with various components such as second harmonic.

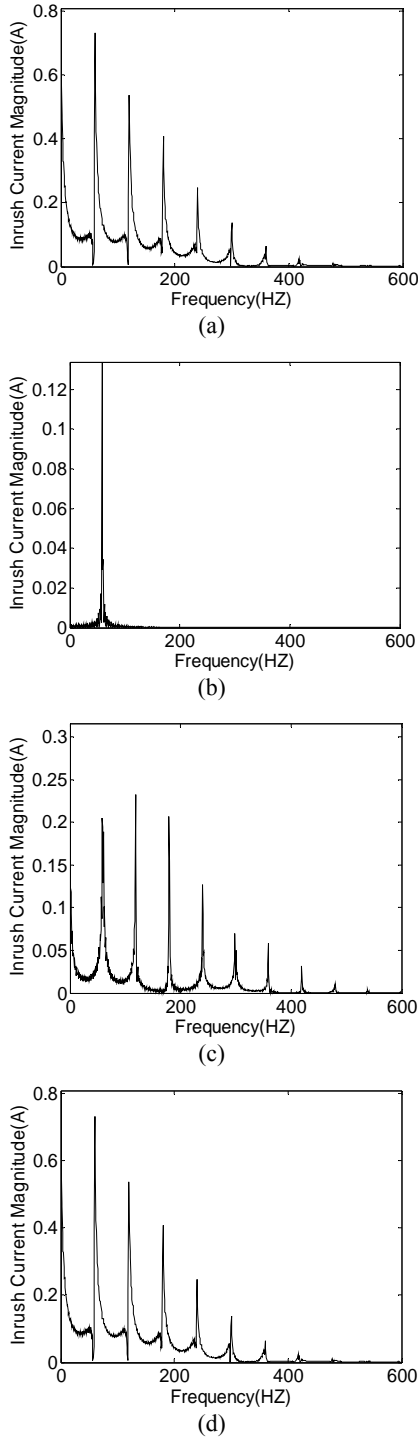


Fig. 8 Inrush current magnitude in the frequency domain for α equal to (a) 90° , (b) 0° , (c) 42.97° , (d) 270° .

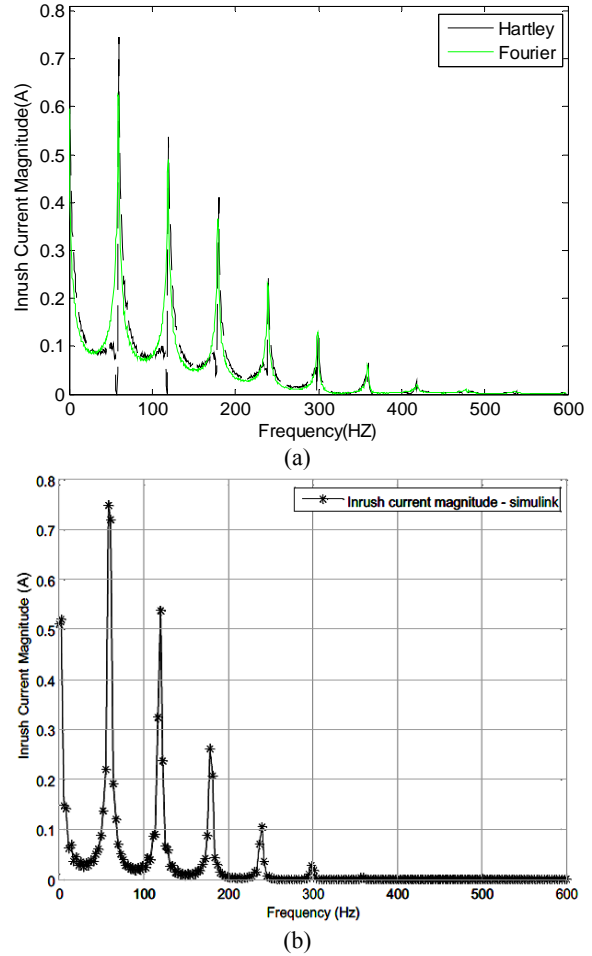


Fig. 9 Inrush current magnitude comparison at 90° between (a) Hartley and Fourier transforms results via Matlab code and (b) FFT result in Simulink.

Table 1 Maximum inrush current magnitudes obtained using Hartley and Fourier transforms.

α (deg.)	Hartley Transform	Fourier Transform
0	0.1338	0.0949
42.97	0.2325	0.2992
45	0.2609	0.3271
90	0.7463	0.6830
135	0.3854	0.3024
180	0.1338	0.0949
225	0.2609	0.3271
270	0.7463	0.6830

The results for 90° using Hartley transform is compared with Fourier transform via Matlab code and also with FFT in Simulink as shown in Fig. 9. We can conclude that Hartley transform gives the best curve with high accuracy and the highest speed of calculation as the time of simulation for this transform is about 6 seconds less than Fourier transform. Table 1 shows the maximum magnitude of inrush current at different voltage angles for both of transforms. The results show negligible difference in the two magnitudes obtained for each angle.

4.2 Three-Phase Three-Limb Transformers

The method is now applied to the analysis of three-phase three-limb transformers, where the magnetic circuits shown in Figs. 10 and 11 are used. The majority of three phase transformers are mostly in the form of core-type construction. Three-limb core-type transformer consists of a single three-phase transformer which is wound on a common magnetic core and uses the least amount of core material in comparison with transformer banks. Under balanced conditions, the three phases have their three respective currents which are displaced 120° from each other. Accordingly, the flux vectors in three phases are displaced 120° apart and summed to zero in the yoke. There is no need for a return path for the flux. This condition is true when the supply voltage is balanced and hence residual flux (i.e. the sum all the three phases) is zero. The electromagnetic behavior of three-phase multi-limb transformers relies on the magnetic interactions and nonlinearities in the ferromagnetic iron-core structure [12–16]. Fig. 12 shows one phase of transformer with open circuited secondary. Calculations are complicated owing to the mutual coupling between the different limbs. Considering the mutual induction of fluxes in three-limb transformer, the equation, vectors and matrices can be written as:

$$V_s(t) = RI(t) + L \frac{dI(t)}{dt} + \frac{d\Psi(t)}{dt} \quad (16)$$

where:

$$\begin{aligned} V_s(t) &= [v_{s1}(t) \quad v_{s2}(t) \quad v_{s3}(t)]^T \\ I(t) &= [i_{inr1}(t) \quad i_{inr2}(t) \quad i_{inr3}(t)]^T \\ \Psi(t) &= [\psi_1(t) \quad \psi_2(t) \quad \psi_3(t)]^T \end{aligned} \quad (17)$$

represent the vectors of input voltages, currents and fluxes, respectively, of the transformer.

Matrices of the winding resistances and inductances are defined as:

$$R = \begin{bmatrix} r_1 & 0 & 0 \\ 0 & r_2 & 0 \\ 0 & 0 & r_3 \end{bmatrix}, \quad L = \begin{bmatrix} L_{11} & m_{12} & m_{13} \\ m_{21} & L_{22} & m_{23} \\ m_{31} & m_{32} & L_{33} \end{bmatrix} \quad (18)$$

The inductance matrix for a three-limb transformer is derived here with the help of its reluctance model in Fig. 11, so the relationship between the fluxes ($\{\phi\}$) and the resultant mmfs ($\{F\}$) should be explicitly derived in terms of the legs reluctances ($\{Rel\}$). Air flux paths and corresponding inductances are not considered for simplicity while deriving the reluctance model. The equations for the reluctance model are:

$$-F_1 + Rel_1\phi_1 + F_2 - Rel_2\phi_2 = 0 \quad (19)$$

$$-F_2 + Rel_2\phi_2 + F_3 - Rel_3\phi_3 = 0 \quad (20)$$

$$\phi_1 + \phi_2 + \phi_3 = 0 \quad (21)$$

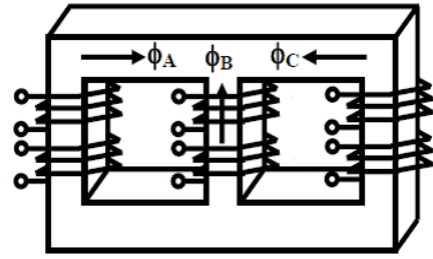


Fig. 10 Three-phase three-limb transformer.

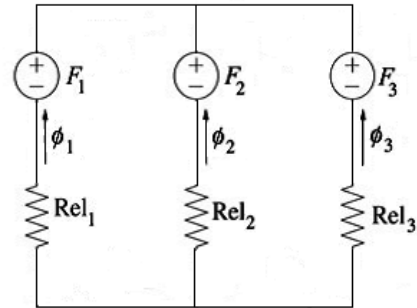


Fig. 11 Representation of three-limb transformer using reluctance network.

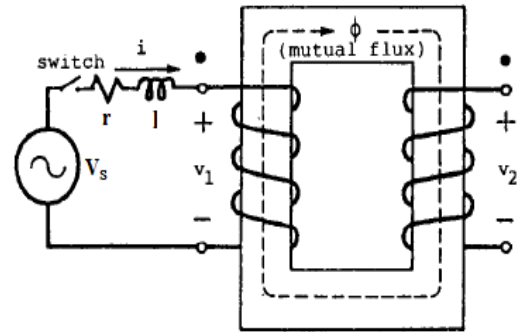


Fig. 12 Per-phase of three-limb transformer.

where $F_1 = N_1 I_1$, $F_2 = N_2 I_2$, $F_3 = N_3 I_3$ and N_1 , N_2 , and N_3 are the turns. Solving Eqs. (19), (20), (21) and assuming that,

$$\Psi_1 = N_1 \phi_1, \quad \Psi_2 = N_2 \phi_2, \quad \Psi_3 = N_3 \phi_3 \quad (22)$$

yields:

$$\Psi_1 = \frac{N_1^2 (Rel_2 + Rel_3) I_1 - N_1 N_2 Rel_3 I_2 - N_1 N_3 Rel_2 I_3}{Rel_1 Rel_2 + Rel_1 Rel_3 + Rel_2 Rel_3} \quad (23)$$

$$\Psi_2 = \frac{N_2^2 (Rel_1 + Rel_3) I_2 - N_1 N_2 Rel_3 I_1 - N_2 N_3 Rel_1 I_3}{Rel_1 Rel_2 + Rel_1 Rel_3 + Rel_2 Rel_3} \quad (24)$$

$$\Psi_3 = \frac{N_3^2 (Rel_1 + Rel_2) I_3 - N_1 N_3 Rel_2 I_1 - N_2 N_3 Rel_1 I_2}{Rel_1 Rel_2 + Rel_1 Rel_3 + Rel_2 Rel_3} \quad (25)$$

Assuming that,

$$N_1 = N_2 = N_3 = N, \text{ Rel}_1 = \text{Rel}_3 \quad (26)$$

and

$$\psi_1 = L_{11}I_1 + m_{12}I_2 + m_{13}I_3 \quad (27)$$

$$\psi_2 = m_{21}I_1 + L_{22}I_2 + m_{23}I_3$$

$$\psi_3 = m_{31}I_1 + m_{32}I_2 + L_{33}I_3$$

gives:

$$L_{11} = L_{33} = \frac{N^2(\text{Rel}_1 + \text{Rel}_2)}{\text{Rel}_1^2 + 2\text{Rel}_1\text{Rel}_2} \quad (28)$$

$$L_{22} = \frac{2N^2\text{Rel}_1}{\text{Rel}_1^2 + 2\text{Rel}_1\text{Rel}_2} \quad (29)$$

$$m_{12} = m_{21} = m_{23} = m_{32} = \frac{-N^2\text{Rel}_1}{\text{Rel}_1^2 + 2\text{Rel}_1\text{Rel}_2} \quad (30)$$

$$m_{13} = m_{31} = \frac{-N^2\text{Rel}_2}{\text{Rel}_1^2 + 2\text{Rel}_1\text{Rel}_2} \quad (31)$$

In the following equations L_{11} , L_{22} and L_{33} have been written l_1 , l_2 and l_3 respectively for simplicity. After obtaining the values of inductances and discretization of the electrical circuit equations under no-load condition we have the following matrix:

$$\begin{bmatrix} r_1\Delta t + l_1 & m_{12} & m_{13} & 1 & 0 & 0 \\ m_{21} & r_2\Delta t + l_2 & m_{23} & 0 & 1 & 0 \\ m_{31} & m_{32} & r_3\Delta t + l_3 & 0 & 0 & 1 \\ 1 & 0 & 0 & \frac{-1}{r_{\text{mag}}\Delta t} & 0 & 0 \\ 0 & 1 & 0 & 0 & \frac{-1}{r_{\text{mag}}\Delta t} & 0 \\ 0 & 0 & 1 & 0 & 0 & \frac{-1}{r_{\text{mag}}\Delta t} \end{bmatrix} \quad (32)$$

$$\times \begin{bmatrix} i_{\text{inr1}}(t + \Delta t) \\ i_{\text{inr2}}(t + \Delta t) \\ i_{\text{inr3}}(t + \Delta t) \\ \psi_1(t + \Delta t) \\ \psi_2(t + \Delta t) \\ \psi_3(t + \Delta t) \end{bmatrix} =$$

$$\begin{bmatrix} v_{s1}(t)\Delta t + l_1 i_{\text{inr1}}(t) + m_{12} i_{\text{inr2}}(t) + m_{13} i_{\text{inr3}}(t) + \psi_1(t) \\ v_{s2}(t)\Delta t + m_{21} i_{\text{inr1}}(t) + l_2 i_{\text{inr2}}(t) + m_{23} i_{\text{inr3}}(t) + \psi_2(t) \\ v_{s3}(t)\Delta t + m_{31} i_{\text{inr1}}(t) + m_{32} i_{\text{inr2}}(t) + l_3 i_{\text{inr3}}(t) + \psi_3(t) \\ i_{\psi_1}(t) - \frac{\psi_1(t)}{r_{\text{mag}}\Delta t} \\ i_{\psi_2}(t) - \frac{\psi_2(t)}{r_{\text{mag}}\Delta t} \\ i_{\psi_3}(t) - \frac{\psi_3(t)}{r_{\text{mag}}\Delta t} \end{bmatrix}$$

Representation of the above matrices in the frequency domain, using Hartley transform, gives:

$$\begin{bmatrix} r_1 + l_1 v & m_{12} v & m_{13} v & v & 0 & 0 \\ m_{21} v & r_2 + l_2 v & m_{23} v & 0 & v & 0 \\ m_{31} v & m_{32} v & r_3 + l_3 v & 0 & 0 & v \\ 1 & 0 & 0 & \frac{-v}{r_{\text{mag}}} & 0 & 0 \\ 0 & 1 & 0 & 0 & \frac{-v}{r_{\text{mag}}} & 0 \\ 0 & 0 & 1 & 0 & 0 & \frac{-v}{r_{\text{mag}}} \end{bmatrix} \times \begin{bmatrix} I_{\text{inr1}}(v) \\ I_{\text{inr2}}(v) \\ I_{\text{inr3}}(v) \\ \Psi_1(v) \\ \Psi_2(v) \\ \Psi_3(v) \end{bmatrix} = \begin{bmatrix} \int v_{s1}(t) (\cos(vt) + \sin(vt)) dt + \psi_1(0) \\ \int v_{s2}(t) (\cos(vt) + \sin(vt)) dt + \psi_2(0) \\ \int v_{s3}(t) (\cos(vt) + \sin(vt)) dt + \psi_3(0) \\ \int i_{\psi_1}(t) (\cos(vt) + \sin(vt)) dt - \frac{\psi_1(0)}{r_{\text{mag}}} \\ \int i_{\psi_2}(t) (\cos(vt) + \sin(vt)) dt - \frac{\psi_2(0)}{r_{\text{mag}}} \\ \int i_{\psi_3}(t) (\cos(vt) + \sin(vt)) dt - \frac{\psi_3(0)}{r_{\text{mag}}} \end{bmatrix} \quad (33)$$

Equations for the fluxes are as follows:

$$\phi_a = \Phi_{\text{max}} \cos(\omega t) \quad (34)$$

$$\phi_b = \Phi_{\text{max}} \cos\left(\omega t - \frac{2\pi}{3}\right)$$

$$\phi_c = \Phi_{\text{max}} \cos\left(\omega t + \frac{2\pi}{3}\right)$$

Parameters of the transformer are considered as, $S = 4.5 \text{ kVA}$, $f = 60 \text{ Hz}$, $r_1 = 0.192 \Omega$, $l_1 = l_3 = 0.9 \text{ mH}$, $l_2 = 1.2 \text{ mH}$, $m_{12} = m_{23} = -0.6 \text{ mH}$, $m_{13} = -0.3 \text{ mH}$, $r_{\text{mag}} = 612.86 \Omega$.

Transformer voltages for an angle of α degree are:

$$V_A = 110 \cos(\omega t - \alpha) \quad (35)$$

$$V_B = 110 \cos\left(\omega t - \left(\frac{2\pi}{3} + \alpha\right)\right)$$

$$V_C = 110 \cos\left(\omega t - \left(\frac{4\pi}{3} + \alpha\right)\right)$$

Switching at zero of the voltage waveform ($\alpha = 90^\circ$) for one phase, results in voltage magnitudes which are 0.866 and -0.866 of the maximum voltage for the other phases, flux will have the maximum value in one phase and half of that for the other phases. If switching occurs at the voltage peak ($\alpha = 0^\circ$), there will be no inrush current for that phase. Distribution of the fluxes in transformer limbs is significant. The transformer secondary is assumed to be open without any load, accordingly the transformer inrush currents in the time domain under zero residual flux condition for switching at $\alpha = 90^\circ$ are exposed in Fig. 13. Low Saturation in the phases B and C results in the less current value. Hysteresis loops for different phases at $\alpha = 90^\circ$ are shown in Fig. 14 and it can be seen that asymmetries in

the hysteresis loops of phases B and C considerably differs from phase A.

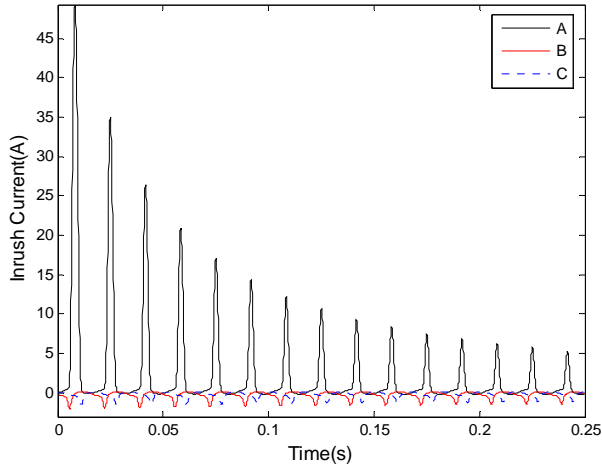


Fig. 13 Three-limb transformer inrush currents for switching at $\alpha = 90^\circ$ for phases A, B and C.

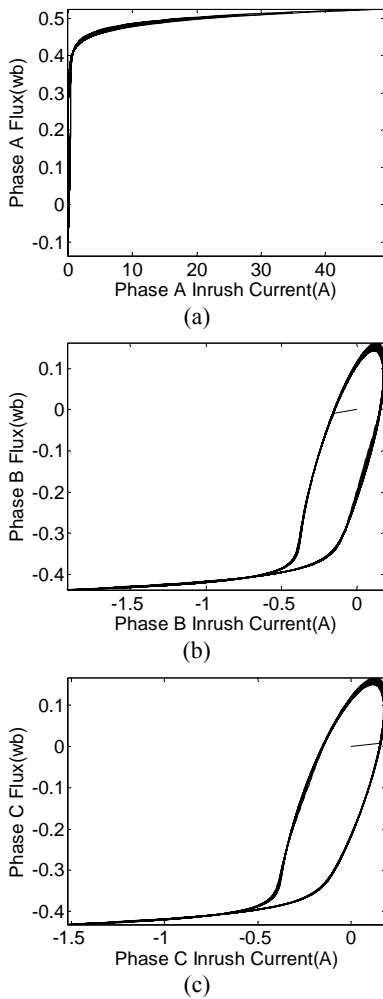


Fig. 14 Hysteresis loops for switching at $\alpha = 90^\circ$ for phases A, B and C.

Fig. 15 shows the transformer inrush current magnitude in the frequency domain using Hartley and Fourier transforms. It can be observed that the magnitude of the inrush current harmonic components varies for phases A, B and C and it has the maximum value in phase A. The second harmonic component is the most dominant one owing to the asymmetrical nature of the magnetizing inrush current. The rise of inrush current harmonic contents in this transformer is more than transformer banks due to the mutual induction of fluxes between the different limbs. The results derived from the figure can also show slight and negligible differences in the inrush current magnitudes for Hartley and Fourier methods. Table 2 shows the time of simulation via Matlab code for both of the transforms which indicates that Harley transform possesses less time compared to Fourier transform for single and three-phase transformers.

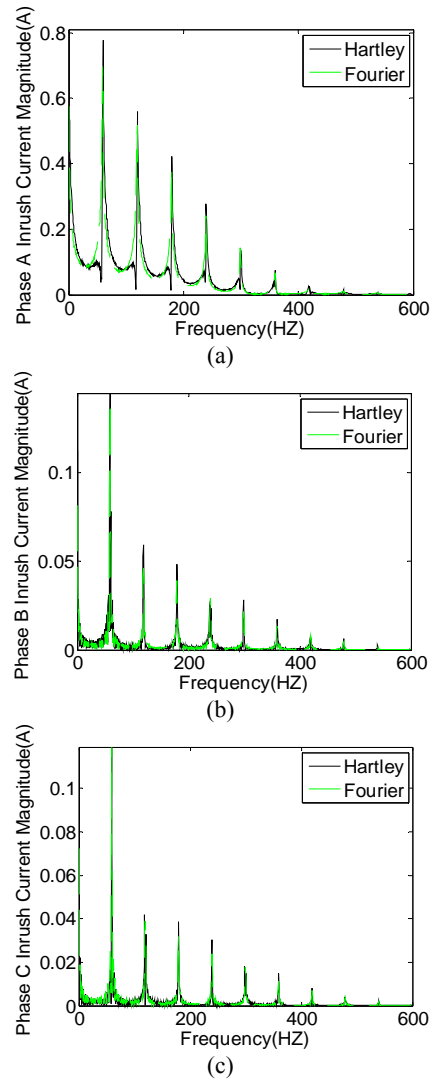


Fig. 15 Three-limb transformer inrush current magnitude comparison between Hartley and Fourier transforms for switching at $\alpha = 90^\circ$ for phases (a) A, (b) B and (c) C.

Table 2 Simulation time for Hartley and Fourier methods.

Transformer Type	Hartley Transform	Fourier Transform
Single-Phase	9 (sec)	15 (sec)
Three-Phase Three-Limb	14 (sec)	21 (sec)

5 Conclusion

Calculation and simulation of inrush current based on operational matrices and Hartley transform are discussed in this paper, considering the problems of the previous methods. The proposed approach simplifies the solution process of a complicated technique without losing accuracy and solves the inrush transients efficiently. It is also appropriate for digital computers and the solution is a multi-resolution type. Performing simultaneous calculations in the time and frequency domain with high efficacy and decreasing the number of computations are the other features of this method. Proper circuits which can consider the nonlinear characteristic and core loss effects are used in this paper. To calculate inrush current using this method, differential equations are first converted into algebraic ones and then Hartley transform which involves no complex quantities or calculations is used to represent equations in the frequency domain. In order to identify the inrush phenomenon owing to switching operation, analysis and simulation of the problem in single-phase and three-phase three-limb transformers are provided in this paper. From the results, it is obvious that the inrush current amplitude increases by lessening the angle to zero of the voltage waveform (or increasing the switching angle α) in single-phase transformers. The results obtained using Hartley transform are also compared with Fourier transform via Matlab code and also with FFT in Matlab Simulink. The method has been executed successfully in three-limb transformer simulations under no-load condition and the results indicate that the inrush current harmonic contents in this transformer depend on the mutual induction of fluxes between the different limbs. This approach can be implemented for computing inrush current in five-limb transformers in future works. It can also provide the basis for reducing inrush via some strategies such as magnetic modifications considering the residual flux.

References

[1] D. I. Taylor, J. D. Law, B. K. Johnson and N. Fischer, "Single-Phase transformer inrush current reduction using prefluxing", *IEEE Transactions on Power Delivery*, Vol. 27, No. 1, pp. 245–252, Jan. 2012.

[2] J. Faiz, B. M. Ebrahimi and T. Noori, "Three and two dimensional finite element computation of

inrush current and short-circuit electromagnetic forces on windings of a three-phase core-type power transformer", *IEEE Transactions on Magnetics*, Vol. 44, No. 5, pp. 590–597, May. 2008.

- [3] L. C. Wu, C. W. Liu, S. E. Chien and C. S. Chen, "The effect of inrush current on transformer protection", *38th North American Power Symposium (NAPS'06)*, pp. 449–456, Sep. 2006.
- [4] J. J. Rico, E. Acha and M. Madrigal, "The study of inrush current phenomenon using operational matrices", *IEEE Transactions on Power Delivery*, Vol. 16, No. 2, pp. 231–237, Apr. 2001.
- [5] A. Semlyen, E. Acha and J. Arrillaga, "Newton-type algorithms for the harmonic phasor analysis of nonlinear power circuits in periodical steady state with special reference to magnetic nonlinearities", *IEEE Transactions on Power Delivery*, Vol. 3, No. 3, pp. 1090–1098, July 1988.
- [6] M. Jamali, M. Mirzaie and S. A. Gholamian, "Calculation and analysis of transformer inrush current based on parameters of transformer and operating conditions", *Electronics and Electrical Engineering (Elektronika Ir Elektrotechnika)*, Vol. 109, No. 3, pp. 17–20, Mar. 2011.
- [7] T. Sridevi, K. R. Reddy and N. L. J. Syamala, "Harmonic analysis of inrush current using fast fourier transform", *International Conference on Power, Energy and Control (ICPEC'13)*, pp. 520–524, Feb. 2013.
- [8] D. Jiandong, W. Chang and Y. Jianming, "Study of the inrush current identification using the improved half-cycle Fourier analysis", *Asia-Pacific Power and Energy Engineering Conference*, pp. 1–4, Mar. 2009.
- [9] J. J. R. Melgoza, G. T. Heydt, A. Keyhani, B. L. Agrawal and D. Selin, "Synchronous machine parameter estimation using the Hartley series", *IEEE Transactions on Energy Conversion*, Vol. 16, No. 1, pp. 49–54, Mar. 2001.
- [10] A. K. Singh, V. K. Singh and O. P. Singh, "The Bernstein operational matrix of integration", *Applied Mathematical Sciences*, Vol. 3, No. 49, pp. 2427–2436, 2009.
- [11] N. Sundararajan, "Fourier and Hartley transforms-A mathematical twin", *Indian Journal of Pure and Applied Mathematics*, Vol. 28, No. 10, pp. 1361–1365, Oct. 1997.
- [12] J. Wang and R. Lascu, "Zero sequence circuit of three-legged core type transformers", *Annual Conference for Protective Relay Engineers*, pp. 188–213, Apr. 2009.
- [13] M. Persson and W. Baig, "Modeling and measurements of transformer behavior at different voltages and frequencies", *Chalmers University of Technology*, pp. 1–58, 2011.

- [14] P. S. Moses, M. A. S. Masoum and M. Moghbel, "Effects of iron-core topology on inrush currents in three-phase multi-leg power transformers", *IEEE Power and Energy Society General Meeting*, pp. 1–6, Jul. 2012.
- [15] S. G. Abdulsalam, W. Xu and V. Dinavahi, "Modelling and simulation of three phase transformers for inrush current studies", *IEE Proc. Generation, Transmission and Distribution*, Vol. 152, No. 3, pp. 328–333, May 2005.
- [16] M. Jamali, M. Mirzaie and S. Gholamian, "Discrimination of inrush from fault currents in power transformers based on equivalent instantaneous inductance technique coupled with finite element method", *Iranian Journal of Electrical and Electronic Engineering*, Vol. 7, No.3, pp. 197-202, Sep. 2011.



Mohammad Ali Taghikhani was born in Tehran, Iran, in 1974. He received the B.Sc. and M.Sc. degrees in electrical engineering from Amirkabir University of Technology, Tehran, Iran, in 1997 and 2000, respectively and received the Ph.D. degree in electrical engineering from Iran University of Science and Technology, Tehran, Iran, in 2008. He

is currently an assistant professor in the department of engineering, Imam Khomeini International University, Qazvin, Iran. His interests are power transformers, electrical machines, numerical analysis, finite element method, heat transfer and fluid mechanics.



Abdolreza Sheikholeslami was born in Iran. He received the B.Sc. degree from Mazandaran University in 1978. He received the M.Sc. and the Ph.D. degrees from Strathclyde University, UK in 1989. Since 2009 he has been an Associate Professor in the department of Electrical and Computer Engineering, Noshirvani University in Babol. His research interests include Power Electronic, Power Quality, Harmonics, Smart Grids and Renewable Energy.



Zahra Taghikhani was born in Tehran, Iran. She received her B.Sc. degree in electrical engineering from Zanjan University, Zanjan, Iran, in 2011 and her M.Sc. degree in electrical engineering from Mazandaran University of Science and Technology, Babol, Iran, in 2014. Her research interests include electrical machines and power transformers.